frontiers | Frontiers in Marine Science

TYPE Original Research
PUBLISHED 28 December 2022
DOI 10.3389/fmars.2022.1097594

OPEN ACCESS

EDITED BY
Bin Wu,
Zhejiang University, China

REVIEWED BY
Hao Gao,
Jinan University, China
Youmin Ying,
Zhejiang University of Technology, China
Junfeng Wang,
South China Sea Institute of Oceanology (CAS), China
Bin-Gui Wang,
Institute of Oceanology (CAS), China

*CORRESPONDENCE
Ling Liu
liul@im.ac.cn

SPECIALTY SECTION
This article was submitted to Marine Biotechnology and Bioproducts, a section of the journal Frontiers in Marine Science

RECEIVED 14 November 2022
ACCEPTED 12 December 2022
PUBLISHED 28 December 2022

CITATION
Huo R, Zhang J, Niu S and Liu L (2022) New prenylated indole diketopiperazine alkaloids and polyketides from the mangrove-derived fungus *Penicillium* sp. *Front. Mar. Sci.* 9:1097594. doi: 10.3389/fmars.2022.1097594

New prenylated indole diketopiperazine alkaloids and polyketides from the mangrove-derived fungus *Penicillium* sp.

Ruiyun Huo[1,2], Jinxin Zhang[1,2], Shubin Niu[3] and Ling Liu[1,2]*

[1]State Key Laboratory of Mycology, Institute of Microbiology, Chinese Academy of Sciences, Beijing, China, [2]College of Life Sciences, University of Chinese Academy of Sciences, Beijing, China, [3]School of Biological Medicine, Beijing City University, Beijing, China

Two new prenylated indole diketopiperazine alkaloids (PIDAs) penicamides A and B (**1** and **2**) and three new polyketides penicinones A–C (**6**–**8**), along with four known compounds deoxybrevianamide E (**3**), brevianamide V (**4**), 12,13-dehydroprolyl-2-(1,1-dimethylallyltryptophyl)diketopiperazine (**5**), and 4-hydroxyphenethyl 2-(4-hydroxyphenyl)acetate (**9**), were isolated and identified from the culture extract of the mangrove-derived fungus *Penicillium* sp. Their structures were fully elucidated by analyzing spectroscopic data. The absolute configurations of these compounds were determined by the comparison of experimental and calculated electronic circular dichroism (ECD) data and $Mo_2(OAc)_4$-induced and $Rh_2(OCOCF_3)_4$-induced ECD experiments. Structurally, compound **1** is the first example of PIDAs featuring a 6/5/8/6/5 pentacyclic ring system with an α-hydroxy group at C-11, while compound **2** is a new analogue of PIDAs possessing the unique 3-methyleneindolin-2-ol moiety. In addition, compound **6** is a new lactone with the furo[3,4-*b*]pyran-5-one moiety. Compound **6** displayed potent cytotoxicity against murine melanoma (B16) cells, human breast adenocarcinoma (MCF-7) cells, and human hepatocellular carcinoma (HepG2) cells at 50.0 μM with inhibitory ratios of 82.7%, 75.1% and 95.9%, respectively. In addition, compound **6** exhibited significantly cytotoxic activity against the HepG2 cells, with an IC_{50} value of 3.87 ± 0.74 μM.

KEYWORDS

***Penicillium* sp., mangrove rhizospheric soil, fungus, secondary metabolites, cytotoxic activity**

Introduction

Fungi have been proven to produce a variety of secondary metabolites possessing significantly biological activities (Guo et al., 2020; Newman and Cragg, 2020; Carroll et al., 2022). Since the discovery of penicillin, cyclosporine, and statins, fungal natural products have made irreplaceable contributions to the development of medicine and human health (Bills

and Gloer, 2016). In recent years, fungi from a mangrove environment, as plant mutualists, parasitizing the tropical and subtropical intertidal forest wetlands, are considered to be a new source of distinctive secondary metabolites with interesting biological activities (Xu, 2015; Carroll et al., 2022; Chen et al., 2022; Zhu et al., 2022). The fungal genus *Penicillium* is one of the most filamentous fungi widely distributed in terrestrial and marine habitats and contains more than 483 known species (Perrone and Susca, 2017; Houbraken et al., 2020). Among them, the mangrove-derived fungi of the genus *Penicillium* are prolific producers of diverse secondary metabolites with a wide range of pharmacological activities (Zhang et al., 2012; Bai et al., 2019; El-Bondkly et al., 2021; Ren et al., 2021), including antitumor agents sumalarin A (Meng et al., 2013) and brocazines A and B (Meng et al., 2014), α-glycosidase inhibitory agents peniisocoumarin C (Cai et al., 2018) and (*R*)-2-chloro-3-(8-hydroxy-6-methoxy-1-oxo-1*H*-isochromen-3-yl)propyl acetate (Qiu et al., 2020), antiviral agent simpterpenoid A (Li et al., 2018), antibacterial agent brevianamide S (Song et al., 2018), and protein tyrosine phosphatase 1B (PTP1B) inhibitory agent penerpene E (Zhou et al., 2019). Genome analyses of the biosynthetic gene clusters have also demonstrated that most of *Penicillium* fungi were biosynthetically talented in producing alkaloids and polyketides (Kozlovskii et al., 2012; Kozlovskii et al., 2015; El Hajj Assaf et al., 2020).

Prenylated indole diketopiperazine alkaloids (PIDAs), featured by tryptophan-containing cyclodipeptides and one or more isoprene units, are an important family of fungal secondary metabolites mainly produced by the genera *Penicillium* and *Aspergillus* (Li, 2010; Peng et al., 2014; Ma et al., 2016). Biogenetically, the skeleton of PIDAs could be derived from the condensation of L-tryptophan with another amino acid catalyzed by a non-ribosomal peptide synthetase, followed by subsequent modifications by tailoring enzymes to form a structural variability of this class of natural products (Ma et al., 2016; Wohlgemuth et al., 2017). PIDAs have also attracted considerable interest from organic chemists due to their high structural diversity with significantly biological activities (Baran and Corey, 2002; Ma et al., 2016; Li et al., 2019; Yang et al., 2021).

In our ongoing studies to search for new bioactive compounds from the mangrove-derived fungi (Liu et al., 2021; Hou et al., 2021; Zhang et al., 2022), the strain *Penicillium* sp. LA032, isolated from the rhizospheric soil of a mangrove ecosystem, was subjected to fermentation on rice. The EtOAc extract showed cytotoxic activity, and its high performance liquid chromatography (HPLC) profiles indicated the presence of abundant secondary metabolites. Then, the large-scale fermentation on rice was performed. The fractionation of the EtOAc extract of this fungus led to the isolation of two new PIDAs penicamides A and B (**1** and **2**), and three new polyketides penicinones A–C (**6**–**8**), along with four known compounds, deoxybrevianamide E (**3**) (Song et al., 2012), brevianamide V (**4**) (Song et al., 2012), 12,13-dehydroprolyl-2-(1,1-dimethylallyltryptophyl)diketopiperazine (**5**) (Steyn, 1973), and 4-hydroxyphenethyl 2-(4-hydroxyphenyl)acetate (**9**) (Wang et al., 2009) (Figure 1). The details of the isolation, structure elucidation, and biological evaluation of these compounds are reported herein. In addition, the proposed biosynthetic pathways of compounds **1**–**5** are reported.

Materials and methods

General experimental procedures

The details of the instruments and equipments can be found in the Supplementary Material.

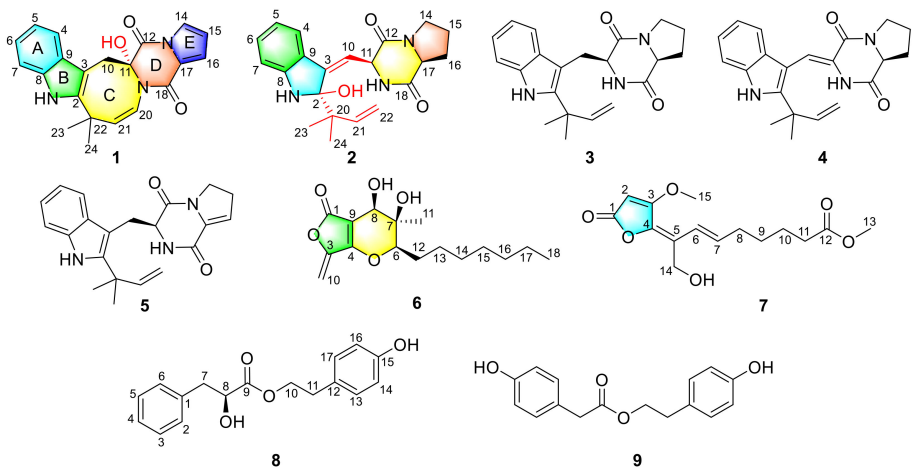

FIGURE 1
Structures of compounds **1**–**9**.

Fungal material

The strain *Penicillium* sp. LA032 was isolated from the rhizospheric soil of a mangrove ecosystem collected from Beilun Estuary, Fangchenggang, Guangxi, People's Republic of China. The fungus LA032 was further identified as *Penicillium* sp. (GenBank Accession No. OP804236), based on a basic local alignment search tool (BLAST) search. The strain was deposited in the laboratory of the Institute of Microbiology, Chinese Academy of Sciences, Beijing.

Fermentation

The strain was firstly cultured on a potato dextrose agar (PDA) medium at 28°C for 7 days. Then, some pieces of agar plugs were cultured on media (1% malt extract, 0.4% yeast extract, and 0.4% glucose) in 500 ml Fernbach flasks at 28°C on a rotary shaker (200 rpm) for 4 days to obtain the seed culture. Finally, the spore inoculums were incubated on 50 × 500 ml Fernbach flasks that contained 100 g of rice and 100 ml of distilled water at room temperature for 21 days.

Extraction and isolation

The fermented products were extracted repeatedly with EtOAc (4 × 6.0 L), which were concentrated to afford 48.0 g of crude residue. The extract was subjected to silica gel column chromatography (CC) eluting with petroleum ether/EtOAc gradient elution to afford eight subfractions Fr.1–Fr.8. Fr.4 (2.1 g) eluted with 30% EtOAc was subjected to silica gel CC with CH_2Cl_2/MeOH to afford Fr.4.1–Fr.4.8. Fr.4.1 (165.3 mg) was further purified by octadecylsilanized (ODS) CC (20%–100% MeOH/H_2O) to yield six subfractions Fr.4.1.1–Fr.4.1.6. Fr.4.1.5 (70.3 mg) eluted with 70% MeOH/H_2O was further purified by reversed-phase (RP) HPLC (57% CH_3CN/H_2O for 60 min; 2.0 ml/min) to afford compound **6** (1.8 mg, t_R 54.0 min). Fr.5 (560.0 mg) eluted with 50% EtOAc was separated by ODS CC using MeOH/H_2O gradient elution to obtain five subfractions Fr.5.1–Fr.5.5. Fr.5.2 (19.0 mg) eluted with 40% MeOH was further purified by RP-HPLC (51% MeOH/H_2O for 50 min; 2.0 ml/min) to get compounds **9** (3.6 mg, t_R 28.5 min) and **8** (1.8 mg, t_R 43.0 min). Fr.7 (630.0 mg) eluted with 80% EtOAc was separated by ODS CC (30%–100% MeOH/H_2O) to afford five subfractions Fr.7.1–Fr.7.5. Fr.7.2 (45.0 mg) was further purified by RP-HPLC (57% MeOH/H_2O for 40 min; 2.0 ml/min) to get compounds **3** (4.8 mg, t_R 26.8 min), **4** (3.8 mg, t_R 28.0 min), and **5** (3.4 mg, t_R 30.2 min). Fr. 7.3 (1.01 g) was subjected to chromatography using a Sephadex LH-20 column (CH_2Cl_2/MeOH, 1:1) to yield six subfractions Fr.7.3.1–Fr.7.3.6. Fr.7.3.3 (30.4 mg) was further purified by RP-HPLC (47% CH_3CN/H_2O for 30 min; 2.0 ml/min) to get compounds **2** (3.1 mg, t_R 21.6 min) and **1** (2.0 mg, t_R 25.0 min). Fr.8 (860.0 mg) eluted with 90% EtOAc was purified by ODS CC eluting with MeOH/H_2O gradient elution to afford seven subfractions Fr.8.1–Fr.8.7. Fr.8.6 (20.6 mg) eluted with 65% MeOH was further purified by RP-HPLC (70% MeOH/H_2O for 30 min; 2.0 ml/min) to get compound **7** (3.1 mg, t_R 28.0 min).

Penicilamide A (***1***): white amorphous powder; $[\alpha]_D^{25}$ +53.3 (*c* 0.06, MeOH); UV (MeOH) λ_{max} (log ϵ) 230 (2.12), 273 (1.56) nm; ECD (*c* 0.82 × 10^{-3} M, MeOH) λ_{max} ($\Delta\epsilon$) 226 (+6.15), 256 (+1.66), 282 (−0.41) nm; IR (neat) ν_{max} 3,343, 2,964, 1,735, 1,636, 1,429, 1,362, and 1,123 cm^{-1}; ^1H and ^{13}C nuclear magnetic resonance (NMR) data, see Table 1; high-resolution electrospray ionisation mass

TABLE 1 | ^1H NMR (500 MHz) and ^{13}C NMR (125 MHz) data for 1 and 2 in acetone-d_6.

Pos.	1		2	
	δ_H (*J* in Hz)	δ_C	δ_H (*J* in Hz)	δ_C
2		142.8, C		98.4, C
3		103.3, C		149.0, C
4	7.53, m	119.0, CH	7.31, d (7.9)	121.9, CH
5	6.92, m	119.7, CH	6.67, td (7.9, 1.1)	119.2, CH
6	6.93, m	121.7, CH	7.06, td (7.9, 1.1)	130.9, CH
7	7.14, m	111.3, CH	6.73, d (7.9)	110.5, CH
8		136.0, C		155.4, CH
9		128.9, C		123.2, C
10	3.54, d (14.8) 3.99, d (14.8)	33.3, CH_2	6.38, d (1.0)	121.1, CH
11		89.0, C	5.26, br s	72.8, CH
12		165.1, C		164.3, C

(Continued)

TABLE 1 Continued

Pos.	1		2	
	δ_H (J in Hz)	δ_C	δ_H (J in Hz)	δ_C
14	7.30, dd (3.5, 1.5)	120.1, CH	3.41, dd (8.5, 5.5)	46.0, CH_2
15	6.31, t (3.5)	116.0, CH	1.90, m	23.5, CH_2
16	6.75, dd (3.5, 1.5)	118.4, CH	2.19, m 2.05, m	28.6, CH_2
17		126.3, C	4.35, t (8.0)	59.4, CH
18		156.9, C		165.7, C
20	6.14, d (8.5)	123.3, CH		50.2, C
21	5.97, d (8.5)	141.9, CH	6.09, dd (17.3, 10.6)	144.2, CH
22		38.4, C	5.02, dd (17.3, 1.3) 4.94, dd (17.3, 1.3)	113.7, CH_2
23	1.57, s	29.3, CH_3	1.13, s	22.8, CH_3
24	1.48, s	33.0, CH_3	1.04, s	23.8, CH_3
1-NH	10.03, br s		6.26, s	

spectrometry (HRESIMS) *m/z* 362.1508 $[M + H]^+$ (calcd for $C_{21}H_{20}N_3O_3$, 362.1505).

Penicilamide B (***2***): white amorphous powder; $[\alpha]_D^{25}$ −140.9 (*c* 0.10, MeOH); UV (MeOH) λ_{max} (log ϵ) 246 (2.60), 333 (1.93) nm; ECD (*c* 0.81 × 10^{-3} M, MeOH) λ_{max} ($\Delta\epsilon$) 234 (+52.3), 266 (−23.7), 341 (−11.3) nm; IR (neat) ν_{max} 3,358, 2,973, 1,667, 1,420, and 1,243 cm^{-1}; ^1H and ^{13}C NMR data, see Table 1; HRESIMS *m/z* 368.1970 $[M + H]^+$ (calcd for $C_{21}H_{26}N_3O_3$, 368.1969).

Penicinone A (***6***): white amorphous powder; $[\alpha]_D^{25}$ −20.0 (*c* 0.10, MeOH); UV (MeOH) λ_{max} (log ϵ) 245 (3.50) nm; ECD (*c* 1.01 × 10^{-3} M, MeOH) λ_{max} ($\Delta\epsilon$) 246 (+31.0), 285 (−17.9) nm; IR (neat) ν_{max} 3,399, 2,955, 2,927, 1,765, 1,644, 1,456, and 1,034 cm^{-1}; ^1H and ^{13}C NMR data, see Table 2; HRESIMS *m/z* 295.1546 $[M - H]^-$ (calcd for $C_{16}H_{23}O_5$, 295.1545).

Penicinone B (***7***): yellow oil; UV (MeOH) λ_{max} (log ϵ) 224 (1.56), 274 (2.05) nm; IR (neat) ν_{max} 3,436, 2,949, 1,735, 1,610, 1,438, and 1,219 cm^{-1}; ^1H and ^{13}C NMR data, see Table 2; HRESIMS *m/z* 297.1332 $[M + H]^+$ (calcd for $C_{15}H_{21}O_6$, 297.1333).

Penicinone C (***8***): colorless oil; $[\alpha]_D^{25}$ −10.0 (*c* 0.10, $CHCl_3$); UV (MeOH) λ_{max} (log ϵ) 217 (2.69), 276 (0.56) nm; ECD (*c* 1.00 × 10^{-3} M, MeOH) λ_{max} ($\Delta\epsilon$) 220 (+1.88) nm; IR (neat) ν_{max} 3,370, 2,958, 1,731, 1,614, 1,516, and 1,225 cm^{-1}; ^1H and ^{13}C NMR data, see Table 2; HRESIMS *m/z* 309.1104 $[M + Na]^+$ (calcd for $C_{17}H_{18}O_4Na$, 309.1103).

$Mo_2(OAc)_4$-induced ECD experiment of 6

The ligand-compound **6** (0.2 mg) was added into a dry solution of $Mo_2(OAc)_4$ (0.7 mg) in dimethyl sulfoxide (DMSO) (400 µl) and was subjected to CD measurements. Firstly, the ECD spectrum was recorded immediately after mixing. Subsequently, its evolution was monitored every 10 min until stationary. Finally, the inherent ECD was subtracted. The diagnostic band observed at ca. 312 nm in the induced ECD spectrum was correlated to the absolute configuration of the 7,8-diol moiety on the basis of Snatzke's regulations (Frelek et al., 1997).

$Rh_2(OCOCF_3)_4$-induced ECD experiment of 8

Compound **8** (0.3 mg) was dissolved in a dry solution of the CH_2Cl_2 (500 µl). Then, 0.6 mg of $[Rh_2(OCOCF_3)_4]$ was added. Subsequently, the first induced ECD spectrum was recorded at once. The following spectrum was measured every 5 min for four times. The correlation between the absolute configuration of C-8 secondary alcohol in **8** and the sign of the E band at 350 nm was inferred using the bulkiness rule (Gerards and Snatzke, 1990; Frelek and Szczepek, 1999).

ECD calculations

The ECD calculations were performed as described previously (Zhang et al., 2022). A conformational search was performed using Maestro 10.2 (Ji and Xu, 2021). The conformers were then optimized using the density functional theory method at the B3LYP/6-311G(2d,p) level by the software package

TABLE 2 | ^{1}H NMR (500 MHz) and ^{13}C NMR (125 MHz) data for 6–8 in acetone-d_6.

Pos.	6		7		8	
	δ_H (J in Hz)	δ_C	δ_H (J in Hz)	δ_C	δ_H (J in Hz)	δ_C
1		167.5, C		167.5, C		138.6, C
2			5.56, s	91.9, CH	7.18, m	130.5, CH
3		149.5, C		172.3, C	7.25, m	129.0, CH
4		163.7, C		141.0, C	7.20, m	127.3, CH
5				124.0, C	7.25, m	129.0, CH
6	4.31, br d (11.0)	89.0, CH	6.55, d (15.6)	125.3, CH	7.18, m	130.5, CH
7		72.2, C	6.40, dt (7.0, 15.6)	138.3, CH	3.01, dd (14.0, 5.0) 2.87, dd (14.0, 7.5)	41.4, CH_2
8	4.20, s	66.9, CH	2.27, m	34.0, CH_2	4.35, dd (7.5, 5.0)	72.6, CH
9		105.0, C	1.51, m	29.3, CH_2		175.4, C
10	5.04, d (3.0) 4.99, d (3.0)	91.7, CH_2	1.64, m	25.3, CH_2	4.23, m	66.5, CH_2
11	1.38, s	20.1, CH_3	2.33, m	34.2, CH_2	2.82, t (7.0)	34.8, CH_2
12	1.99, m 1.74, m	29.2, CH_2		174.1, C		129.6, C
13	1.57, m 1.42, m	27.8, CH_2	3.61, s	51.6, CH_3	7.09, dt (8.5, 2.0)	130.9, CH
14	1.30, m	29.5, CH_2	4.64, s	55.6, CH_2	6.79, dt (8.5, 2.0)	116.2, CH
15	1.30, m	29.5, CH_2	4.02, s	60.4, CH_3		157.1, C
16	1.30, m	32.6, CH_2			6.79, dt (8.5, 2.0)	116.2, CH
17	1.30, m	23.4, CH_2			7.09, dt (8.5, 2.0)	130.9, CH
18	0.87, t (7.0)	14.4, CH_3				
7-OH	4.76, s					
8-OH	4.26, s					

Gaussian 09 (Frisch et al., 2013). The 60 lowest energy conformations were calculated by the ECD calculations using the time-dependent density functional theory (TDDFT) methodology at the CAM-B3LYP/6-311G(d,p) level.

Cell viability assay

Cytotoxic assays were conducted as previously described (Liu et al., 2015). The detailed procedure is described in the Supplementary Material.

Results and discussion

Compound isolation and structure elucidation

The fungus *Penicillium* sp. LA032 was fermented on rice solid culture and extracted three times with EtOAc. The EtOAc extract (48.0 g) was fractionated by silica gel vacuum liquid chromatography (VLC), Sephadex LH-20 CC, and semipreparative HPLC to afford five new compounds (**1**, **2** and **6**–**8**) and four known compounds.

Penicilamide A (**1**) was obtained as white amorphous powder. The molecular formula of **1** was determined as $C_{21}H_{19}N_3O_3$ by the HRESIMS molecular ion peak at m/z 362.1508 $[M + H]^+$ (calcd for $C_{21}H_{20}N_3O_3$, 362.1505), indicating 14 degrees of unsaturation. The IR spectrum showed absorption bands at 3,343, 2,964, 1,735, 1,636, and 1,429 cm^{-1}, indicating the presence of amino, hydroxy, carbonyl, and aromatic functional groups. The ^{1}H NMR spectrum (Table 1 and Figure S1) exhibited one exchangeable proton (δ_H 10.03), nine olefinic or aromatic protons (δ_H 7.53, 7.30, 7.14, 6.93, 6.92, 6.75, 6.31, 6.14, and 5.97), one methylene (δ_H 3.99 and 3.54), and two singlet methyls (δ_H 1.57 and 1.48). The ^{13}C NMR spectrum (Figure S2) and heteronuclear single quantum coherence (HSQC) spectrum (Figure S3) showed the

presence of 21 carbon resonances, including two methyls, one methylene, nine olefinic or aromatic methines, and nine quaternary carbons (two sp^3 quaternary carbons at δ_C 38.4 and 73.8; five sp^2 carbons at δ_C 103.3, 126.3, 128.9, 136.0, and 142.8; and two amide carbonyls at δ_C 165.1 and 156.9). Taking the above NMR data and molecular formula into consideration, an aromatic system, four double bonds and two amide carbonyl functionalities accounted for 10 indices of hydrogen deficiency, suggesting that **1** was a pentacyclic compound. The disubstituted indole moiety (rings A and B) in **1** was assigned by the heteronuclear multiple bond correlations (HMBC) correlations (Figures 2 and S5) from H-4 to C-3 (δ_C 103.3), C-6 (δ_C 121.7), C-8 (δ_C 136.0), and C-9 (δ_C 128.9) and from H-7 to C-5 (δ_C 119.7), C-8, and C-9, together with the ^{1}H-^{1}H COSY cross-peaks (Figures 2 and S4) of H-4/H-5/H-6/H-7. The characteristic NMR data of two amide carbonyls (C-12 and C-18: δ_C 165.1 and 156.9, respectively) and the HMBC cross-peaks from H-16 to C-17 (δ_C 126.3) and C-18 and from H-14 to C-17, along with the ^{1}H-^{1}H COSY cross-peaks of H-14/H-15/H-16, permitted the completion of the diketopiperazine ring and the unsaturated proline moiety (rings D and E). The other HMBC correlations from H_2-10 to C-2 (δ_C 142.8), C-3, C-9, C-11 (δ_C 89.0) and C-12, from H-20 to C-18 and C-22 (δ_C 38.4), from H-21 to C-2, and from H_3-23/H_3-24 to C-2, C-21 (δ_C 141.9), and C-22, combined with the ^{1}H-^{1}H COSY cross-peak of H-20/H-21, safely expounded that rings B and D were cyclized at C-20 and a nitrogen atom to form an azocane subunit (ring C), completing the unusual 6/5/8/6/5 pentacyclic ring system. The chemical shift value for C-11 (δ_C 89.0) indicated that the carbon C-11 was substituted by the hydroxyl group, which was also supported by the molecular formula of **1**. Then, the structure of **1** was finally determined.

The absolute configuration for compound **1** was determined unequivocally by the comparison of the experimental and calculated ECD curves. The ECD spectra of 11*R*-(**1a**) and 11*S*-(**1b**) were performed using the time-dependent density functional theory (TD-DFT) at the CAM-B3LYP/6-311G(d,p) level. The calculated ECD spectrum of 11*R*-(**1a**) matched well with the experimental one of **1** (Figure 3), which allowed the assignment of the absolute configuration of **1** as 11*R*.

Penicilamide B (**2**) had a molecular formula of $C_{21}H_{25}N_3O_3$ as deduced from the HRESIMS and ^{13}C NMR data, with 11 degrees of unsaturation, which is 16 mass units higher than that of deoxybrevianamide E (**3**) (Song et al., 2012). The ^{1}H, ^{13}C, and HSQC spectroscopic data (Table 1 and Figures S7–S9) suggested the presence of two methyls, four methylenes (one sp^2 methylene), two sp^3 methines, six olefinic/aromatic methines, and seven quaternary carbons including two amide carbonyls (δ_C 164.3 and 165.7). The ^{1}H NMR and ^{13}C NMR data (Table 1) of **2** were similar to those of the coisolated compound **3**, with slight differences in the chemical shift values of C-2, C-3, C-9, C-10, C-11, and C-20, suggesting their structural similarity. A further analysis of their NMR data indicated that the olefin C-2/C-3 in **3** was replaced by the olefin C-3/C-10 in **2** and an extra hydroxy group was located at C-2 in **2**, as supported by the HMBC correlations (Figures 2 and S11) from 1-NH (δ_H 6.26), H-21, H_3-23, and H_3-24 to the sp^3 quaternary carbon C-2 (δ_C 98.4) and C-20, from H-4 (δ_H 7.31) to the olefinic quaternary carbon C-3 (δ_C 149.0), from H-10 (δ_H 6.38) to C-2, C-3, C-9, C-11, and C-12 and from H-11 (δ_H 5.26) to C-3 and the olefinic methine carbon C-10 (δ_C 121.1), together with the ^{1}H-^{1}H COSY cross-peak (Figures 2 and S10) of H-10/H-11. In the nuclear overhauser effect spectroscopy (NOESY) spectrum (Figures 4 and S12), the NOESY correlation of H-4/H-10 suggested the olefin C-3/C-10 as *Z* geometry. In addition, the cross-peaks of H-11 with H-17 and H_3-24 suggested that these protons were cofacial, implying the existence of two possible configurations 2*R*,11*S*,17*S*-(**2a**) and 2*S*,11*R*,17*R*-(**2b**). Lastly, the absolute configuration of **2** was also established by ECD calculations. The experimental ECD curve was consistent with the calculated one of 2*R*,11*S*,17*S*-(**2a**), indicating the 2*R*,11*S*,17*S* configuration

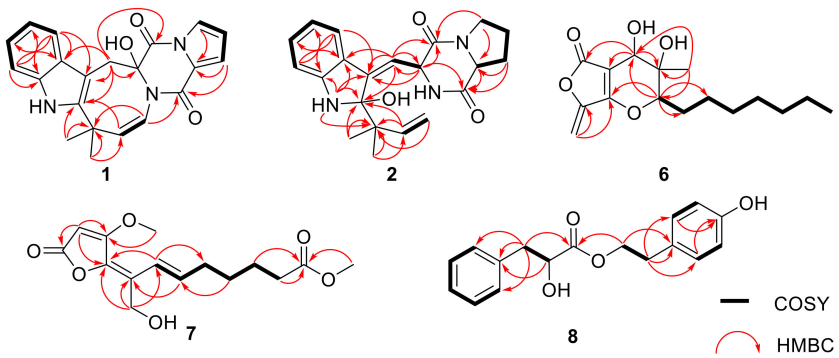

FIGURE 2
Key correlations of compounds **1**, **2**, and **6**–**8**.

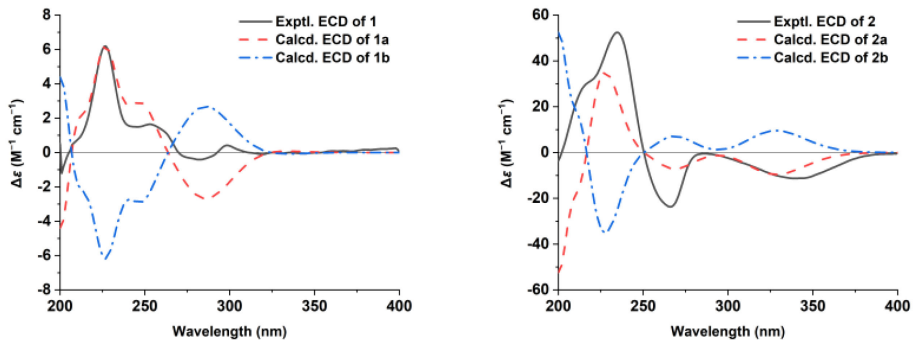

FIGURE 3
The calculated and experimental electronic circular dichroism (ECD) spectra of **1** and **2**.

of **2**. Finally, compound **2** was established as a PIDA featuring a rare 3-methyleneindolin-2-ol moiety.

Penicinone A (**6**), obtained as white amorphous powder, had a molecular formula of $C_{16}H_{24}O_5$ as deduced from the negative HRESIMS peak at *m/z* 295.1546 $[M - H]^-$ (calcd for $C_{16}H_{23}O_5$, 295.1545) and the NMR data (Table 2), implying five indices of hydrogen deficiency. The analysis of the ^1H, ^{13}C, and HSQC spectra (Table 2 and Figures S13–S15) showed the presence of two methyls, six sp^3 methylenes, one sp^2 methylene ($\delta_{C/H}$ 91.7/4.02, 5.04), two oxygenated methines ($\delta_{C/H}$ 89.0/4.31 and 66.9/4.20), one sp^3 quaternary carbon (δ_C 72.2), three sp^2 quaternary carbons, and one carbonyl (δ_C 167.5). The NMR data of **6** were almost similar to those of isoaigialone B (Silva et al., 2017) except that one oxygenated methine and one methyl group were absent, while the exocyclic double bond ($\delta_{C/H}$ 91.7/4.99, 5.04; δ_C 149.5) signals were observed in **6**. The HMBC correlations (Figures 2 and S17) from H_2-10 (δ_H 4.99, 5.04) to C-3 (δ_C 149.5) and C-4 (δ_C 163.7) further confirmed the existence of an exocyclic double bond at C-3 and C-10 positions of **6**. A comprehensive analysis of the ^1H-^1H COSY (Figures 2 and S16) and HMBC correlations corroborated the planar structure of compound **6** with the furo[3,4-*b*]pyran-5-one ring system as shown. The NOESY correlations (Figures 4 and S18) of H_3-11 with H-6 and H-8 suggested that these protons were on the same side of the pyran ring. Furthermore, Snatzke's method was employed to address the absolute configuration of the 7,8-diol unit. After mixing **6** and dimolybdenum tetraacetate $[Mo_2(OAc)_4]$ in DMSO, ECD data were measured between 250 and 450 nm. The inherent ECD was subtracted. The positive Cotton effect (CE) at 312 nm (Figure 5) in the induced spectrum of **6** indicated a 7*R*,8*R* configuration of the 7,8-diol (Frelek et al., 1997; Di Bari et al., 2001). Thus, the absolute configuration of **6** was established as 6*R*,7*R*,8*R*.

Penicinone B (**7**) was obtained as yellow oil. Its molecular formula was deduced as $C_{15}H_{20}O_6$ (six degrees of unsaturation) by the analysis of its HRESIMS and 1D NMR data (Table 2). The interpretation of its IR spectrum indicated the presences of hydroxy (3436 cm^{-1}) and α,β-unsaturated lactone carbonyl (1735 cm^{-1}) functional groups. The analysis of the ^1H, ^{13}C and HSQC NMR data (Table 2 and Figures S19–S21) of **7**

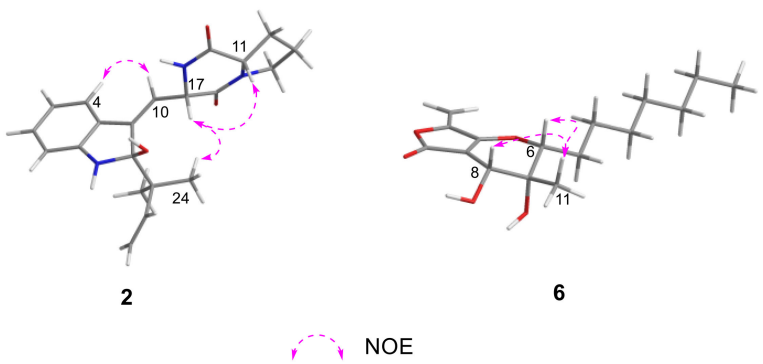

FIGURE 4
Key NOESY correlations of **2** and **6**.

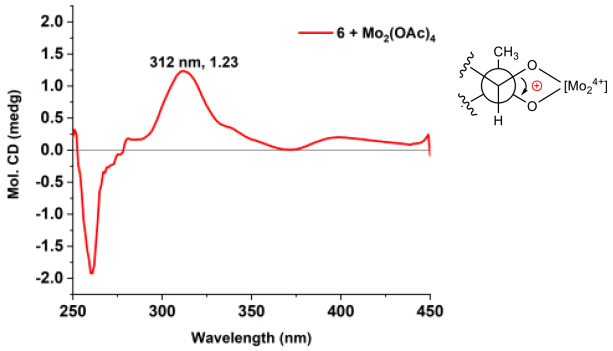

FIGURE 5
ECD spectrum of **6** in DMSO containing $Mo_2(OAc)_4$ with the inherent ECD spectrum subtracted.

revealed the presence of five methylenes (one oxygenated), two methoxy groups ($\delta_{C/H}$ 60.4/4.02 and 51.6/3.61), six olefinic carbons (three protonated), and two ester carbonyl carbons (δ_C 167.5 and 174.1), accounting for five degrees of unsaturation. Therefore, the remaining one unsaturation indicated the presence of a monocyclic ring system in **7**. The characteristic signals of the α,β-unsaturated lactone subunit corresponding to a lactone carbonyl carbon (δ_C 167.5), a quaternary carbon (δ_C 141.0) and two olefinic carbons (δ_C 172.3 and 91.9, respectively), as well as the HMBC correlations (Figures 2 and S23) from H-2 to C-1, C-3 and C-4 and from H_3-15 to C-3, permitted the completion of the 2(5*H*)-furanone moiety with the methoxy carbon C-15 attached at C-3. The ^{1}H-^{1}H COSY cross-peaks (Figures 2 and S22) of H-6/H-7/H_2-8/H_2-9/H_2-10/H_2-11, combined with the HMBC cross-peaks from H_2-10, H_2-11 and H_3-13 to C-12 (δ_C 174.1), established the C-6–C-13 subunit. Furthermore, the HMBC correlations from H-6 to C-4 and C-14, from H-7 to C-5, and from H_2-14 to C-4, C-5 and C-6 demonstrated that both C-6 and C-14 were directly attached to the C-4/C-5 double bond at C-5. The remaining hydroxyl group was substituted at C-14, which are deduced by the chemical shift of C-14 (δ_C 55.6) and the molecular formula of **7**. The large coupling constant of the olefinic protons of H-6 and H-7 (15.6 Hz) suggested the olefin C-6/C-7 as *E* geometry. The NOESY correlation H_3-15 to H-2 and the lack of NOESY cross-peak between H_3-15 and H_2-14 indicated the *Z*-configuration of the C-4/C-5 double bond based on the previous literature (Phainuphong et al., 2017). Therefore, the structure of **7** was established as depicted.

Penicinone C (**8**) was isolated as colorless oil. The molecular formula of **8** was established as $C_{17}H_{18}O_4$ from the positive HRESIMS data (*m/z* 309.1104 $[M + Na]^+$, calcd 309.1103). The ^{1}H and ^{13}C NMR data (Table 2) of **8** were close to those of 4′-hydroxyphenylethyl 4,8(*R*)-dihydroxyphenylpropionate (Sun et al., 2021), except that the hydroxy group at C-4 disappeared in **8**. This observation was supported by the HMBC correlations (Figures 2 and S29) from H_2-7 (δ_H 2.87, 3.01) to C-1 (δ_C 138.6), C-2 (δ_C 130.5), C-6 (δ_C 130.5) and C-9 (δ_C 174.5) and from H-2 (δ_H 7.18) and H-6 (δ_H 7.18) to C-4 (δ_C 127.3), as well as the ^{1}H-^{1}H COSY cross-peaks (Figures 2 and S28) of H-3/H-4/H-5. The absolute configuration of C-8 in **8** was determined by the circular dichroism data of the *in situ* formed $[Rh_2(OCOCF_3)_4]$ complex, with the inherent contribution subtracted (Gerards and Snatzke, 1990; Frelek and Szczepek, 1999). The $Rh_2(OCOCF_3)_4$-induced ECD spectrum of **8** showed positive CE at 350 nm (Figure 6), suggesting the 8*S* configuration (Gerards and Snatzke, 1990; Frelek and Szczepek, 1999). Therefore, the absolute configuration of compound **8** was established as 8*S*.

The structures of four known compounds, deoxybrevianamide E (**3**) (Song et al., 2012), brevianamide V (**4**) (Song et al., 2012), 12,13-dehydroprolyl-2-(1,1-dimethylallyltryptophyl) diketopiperazine (**5**) (Steyn, 1973) and 4-hydroxyphenethyl 2-(4-hydroxyphenyl)acetate (**9**) (Wang et al., 2009) (Figure 1), were

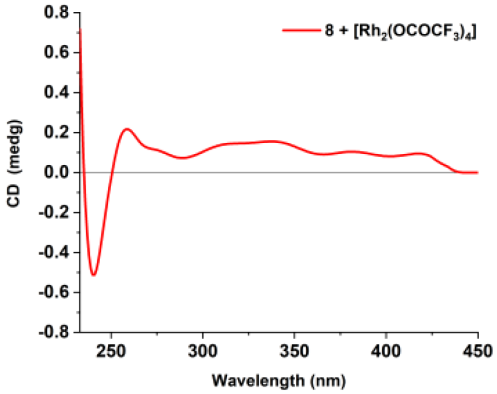

FIGURE 6
ECD spectrum of the $[Rh_2(OCOCF_3)_4]$ complex of compound **8** with the inherent ECD spectrum subtracted.

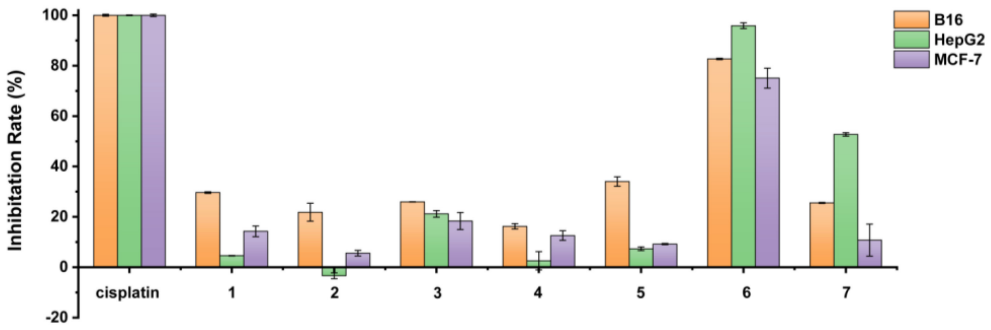

FIGURE 7
Inhibition rate (%) of compounds **1**–**7** on B16, HepG2 and MCF7 cells at 50.0 μM.

assigned by the interpretation of their spectroscopic data with those reported in the literature.

To the best of our knowledge, the PIDAs featuring the 6/5/8/6/5 pentacyclic moiety are rare in nature, with only 10 compounds being reported (Steyn, 1973; Quang et al., 2013; Zhuravleva et al., 2021). Moreover, the hydroxy group is usually located at the C-3, C-16, or C-17 position in these metabolites (Quang et al., 2013; Zhuravleva et al., 2021). Penicilamide A (**1**) represents the first example of PIDAs featuring the unique 6/5/8/6/5 pentacyclic skeleton with an α-hydroxy group at the C-11 position. Meanwhile, penicilamide B (**2**) is a new PIDA with a 3-methyleneindolin-2-ol moiety. Biogenetically, PIDAs **1**–**5** could be derived from the condensation of L-tryptophan with L-proline. The biosynthetic intermediate **I** was firstly produced, followed by reverse C2 prenylation to afford the intermediate **3**. Starting from compound **3**, compounds **1**, **2**, **4**, and **5** could be generated *via* oxidation, dehydrogenation, and cyclization reactions. The plausible biosynthetic pathways were proposed as shown in Scheme 1. In addition, compound **6** was established as a rare furo[3,4-*b*]pyran-5-one skeleton with an *n*-heptyl moiety. Meanwhile, compounds **7** and **8** are γ-butenolide and phenolic acid derivatives, respectively.

Biological activity

Compounds **1**–**7** were tested for their cytotoxic activity against B16 (murine melanoma cells), MCF-7 (human breast adenocarcinoma cells), and HepG2 (human hepatocellular carcinoma cells) at 50.0 μM. Compound **6** displayed potent cytotoxicity against B16, MCF-7, and HepG2 cell lines at 50.0 μM with inhibitory ratios of 82.7%, 75.1%, and 95.9%, respectively (Figure 7). Furthermore, compound **6** showed more potent cytotoxicity against HepG2 cells (IC_{50} value of 3.09 ± 0.03 μM) than that of the positive-control cisplatin (IC_{50} value of 8.71 ± 0.28 μM). Compound **6** also showed cytotoxicity against MCF-7 and B16 cells, with IC_{50} values of 30.01 ± 0.52 and 27.91 ± 0.17 μM, respectively, whereas the positive-control cisplatin showed IC_{50} values of 4.22 ± 0.46 and 20.39 ± 3.25 μM, respectively. Other compounds did not show

TABLE 3 Cytotoxicity data of compounds 1–7 against the tumor cell lines.

Compounds	Cell lines (μM)		
	B16	HepG2	MCF-7
1	>50	>50	>50
2	>50	>50	>50
3	>50	>50	>50
4	>50	>50	>50
5	>50	>50	>50
6	27.91 ± 0.17	3.09 ± 0.03	30.01 ± 0.52
7	>50	>50	>50
Cisplatin	20.39 ± 3.25	8.71 ± 0.28	4.22 ± 0.46

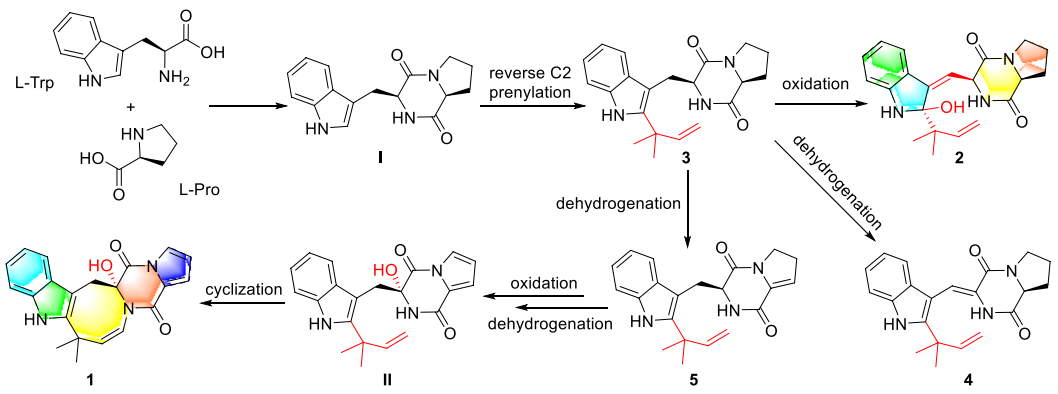

SCHEME 1
Inhibition rate (%) of compounds **1**–**7** on B16, HepG2 and MCF7 cells at 50.0 μM.

obviously inhibitory effects on the cell lines tested at 50.0 μM (Table 3).

Conclusion

In summary, two new PIDAs penicamides A and B (**1** and **2**) and three new polyketides penicinones A–C (**6**–**8**), together with four known compounds, were identified from the mangrove-derived fungus *Penicillium* sp. Compound **1** possesses an unusual 6/5/8/6/5 pentacyclic ring system with an α-hydroxy group at C-11, which was rarely encountered in the PIDAs. Compound **2** is the first reported natural product of PIDAs with a 3-methyleneindolin-2-ol moiety. Compound **6** is a rare furo [3,4-*b*]pyran-5-one skeleton with an *n*-heptyl moiety. Compound **6** exhibited significant cytotoxicity against HepG2 cells, which might be worthy for further pharmacological study and structural modification toward more potent drug leads. These findings not only enriched the chemical space of the PIDA and polyketide families but also provided important hints for the discovery of new drug leads.

Data availability statement

The original contributions presented in the study are included in the article/Supplementary Material. Further inquiries can be directed to the corresponding author/s.

Author contributions

Conceptualization, LL. Methodology, RH. Resources, RH, JZ, and SN. Data curation, RH and JZ. Writing–original draft preparation, RH. Writing–review and editing, RH and LL. Project administration and funding acquisition, LL. All authors contributed to the article and approved the submitted version.

Funding

This research was funded by grants from National Key Research and Development Program of China (2021YFC2100600) and the National Natural Science Foundation of China (32022002 and 21977113).

Conflict of interest

The authors declare that the research was conducted in the absence of any commercial or financial relationships that could be construed as a potential conflict of interest.

Publisher's note

Supplementary material

The Supplementary Material for this article can be found online at: https://www.frontiersin.org/articles/10.3389/fmars.2022.1097594/full#supplementary-material

References

Bai, M., Zheng, C. J., Huang, G. L., Mei, R. Q., Wang, B., Luo, Y. P., et al. (2019). Bioactive meroterpenoids and isocoumarins from the mangrove-derived fungus *Penicillium* sp. TGM112. *J. Nat. Prod.* 82, 1155–1164. doi: 10.1021/acs.jnatprod.8b00866

Baran, P. S., and Corey, E. J. (2002). A short synthetic route to (+)-austamide, (+)-deoxyisoaustamide, and (+)-hydratoaustamide from a common precursor by a novel palladium-mediated indole → dihydroindoloazocine cyclization. *J. Am. Chem. Soc* 124, 7904–7905. doi: 10.1021/ja026663t

Bills, G. F., and Gloer, J. B. (2016). Biologically active secondary metabolites from the fungi. *Microbiol. Spectr.* 4, 1–32. doi: 10.1128/microbiolspec.FUNK-0009-2016

Cai, R. L., Wu, Y. N., Chen, S. H., Cui, H., Liu, Z. M., Li, C. Y., et al. (2018). Peniisocoumarins A-J: Isocoumarins from *Penicillium commune* QQF-3, an endophytic fungus of the mangrove plant *Kandelia candel*. *J. Nat. Prod.* 81, 1376–1383. doi: 10.1021/acs.jnatprod.7b01018

Carroll, A. R., Copp, B. R., Davis, R. A., Keyzers, R. A., and Prinsep, M. R. (2022). Marine natural products. *Nat. Prod. Rep.* 39, 1122–1171. doi: 10.1039/D1NP00076D

Chen, S. H., Cai, R. L., Liu, Z. M., Cui, H., and She, Z. G. (2022). Secondary metabolites from mangrove-associated fungi: source, chemistry and bioactivities. *Nat. Prod. Rep.* 39, 560–595. doi: 10.1039/D1NP00041A

Di Bari, L., Pescitelli, G., Pratelli, C., Pini, D., and Salvadori, P. (2001). Determination of absolute configuration of acyclic 1,2-diols with $Mo_2(OAc)_4$. 1. snatzke's method revisited. *J. Org. Chem.* 66, 4819–4825. doi: 10.1021/jo010136v

El-Bondkly, E. A. M., El-Bondkly, A. A. M., and El-Bondkly, A. A. M. (2021). Marine endophytic fungal metabolites: A whole new world of pharmaceutical therapy exploration. *Heliyon* 7, e06362. doi: 10.1016/j.heliyon.2021.e06362

El Hajj Assaf, C., Zetina-Serrano, C., Tahtah, N., Khoury, A. E., Atoui, A., Oswald, I. P., et al. (2020). Regulation of secondary metabolism in the *Penicillium* genus. *Int. J. Mol. Sci.* 21, 9462. doi: 10.3390/ijms21249462

Frelek, J., Ikekawa, N., Takatsuto, S., and Snatzke, G. (1997). Application of [$Mo_2(OAc)_4$] for determination of absolute configuration of brassinosteroid vic-diols by circular dichroism. *Chirality* 9, 578–582. doi: 10.1002/(SICI)1520-636X(1997)9:5/6<578::AID-CHIR27>3.0.CO;2-K

Frelek, J., and Szczepek, W. J. (1999). [$Rh_2(OCOCF_3)_4$] as an auxiliary chromophore in chiroptical studies on steroidal alcohols. *Tetrahedron: Asymmetry* 10, 1507–1520. doi: 10.1016/S0957-4166(99)00115-9

Frisch, M. J., Trucks, G. W., Schlegel, H. B. M., Scuseria, G. E., Robb, M. A., Cheeseman, J. R., et al. (2013). *Gaussian 09, revision e. 01* (Wallingford, CT: Gaussian, Inc).

Gerards, M., and Snatzke, G. (1990). Circular dichroism. XCIII determination of the absolute configuration of alcohols, olefins, epoxides, and ethers rom the CD of their "in situ" complexes with [$Rh_2(O_2CCF_3)_4$]. *Tetrahedron: Asymmetry* 1, 221–236. doi: 10.1016/S0957-4166(00)86328-4

Guo, L. F., Liu, G. R., and Liu, L. (2020). Caryophyllene-type sesquiterpenoids and α-furanones from the plant endophytic fungus *Pestalotiopsis theae*. *Chin. J. Nat. Med.* 18, 261–267. doi: 10.1016/S1875-5364(20)30032-7

Houbraken, J., Kocsubé, S., Visagie, C. M., Yilmaz, N., Wang, X. C., Meijer, M., et al. (2020). Classification of aspergillus, *Penicillium*, *Talaromyces* and related genera (*Eurotiales*): An overview of families, genera, subgenera, sections, series and species. *Stud. Mycol.* 95, 5–169. doi: 10.1016/j.simyco.2020.05.002

Hou, B. L., Liu, S. S., Huo, R. Y., Li, Y. Q., Ren, J. W., Wang, W. Z., et al. (2021). New diterpenoids and isocoumarin derivatives from the mangrove-derived fungus *Hypoxylon* sp. *Mar. Drugs* 19, 362. doi: 10.3390/md19070362

Ji, C. F., and Xu, X. Z. (2021). Recent advancements of macrolide hybrids against *Staphylococcus aureus*. *Curr. Top. Med. Chem.* 21, 2455–2473. doi: 10.2174/1568026620999201203213733

Kozlovskii, A. G., Antipova, T. V., and Zhelifonova, V. P. (2015). Biosynthesis of biologically active low-molecular weight compounds by fungi of the genus *Penicillium* (review). *Appl. Biochem. Microbiol.* 51, 236–242. doi: 10.1134/s0003683815020118

Kozlovskii, A. G., Zhelifonova, V. P., Antipova, T. V., Baskunov, B. P., Kochkina, G. A., and Ozerskaya, S. M. (2012). Secondary metabolite profiles of the *Penicillium* fungi isolated from the arctic and antarctic permafrost as elements of polyphase taxonomy. *Microbiology* 81, 306–311. doi: 10.1134/S0026261712030071

Li, S. M. (2010). Prenylated indole derivatives from fungi: structure diversity, biological activities, biosynthesis and chemoenzymatic synthesis. *Nat. Prod. Rep.* 27, 57–78. doi: 10.1039/b909987p

Liu, L., Chen, X. X., Li, D., Zhang, Y., Li, L., Guo, L. D., et al. (2015). Bisabolane sesquiterpenoids from the plant endophytic fungus *Paraconiothyrium brasiliense*. *J. Nat. Prod.* 78, 746–753. doi: 10.1021/np5009569

Liu, G. R., Niu, S. B., and Liu, L. (2021). Alterchromanone a, one new chromanone derivative from the mangrove endophytic fungus *Alternaria longipes*. *J. Antibiot. (Tokyo)* 74, 152–155. doi: 10.1038/s41429-020-00364-4

Li, H. L., Xu, R., Li, X. M., Yang, S. Q., Meng, L. H., and Wang, B. G. (2018). Simpterpenoid a, a meroterpenoid with a highly functionalized cyclohexadiene moiety featuring gem-propane-1,2-dione and methylformate groups, from the mangrove-derived *Penicillium simplicissimum* MA-332. *Org. Lett.* 20, 1465–1468. doi: 10.1021/acs.orglett.8b00327

Li, H. Q., Xu, D., Sun, W. G., Yang, B. Y., Li, F. L., Liu, M. T., et al. (2019). HPLC-DAD-directed isolation of linearly fused prenylated indole alkaloids from a soil-derived *Aspergillus versicolor*. *J. Nat. Prod.* 82, 2181–2188. doi: 10.1021/acs.jnatprod.9b00183

Ma, Y. M., Liang, X. A., Kong, Y., and Jia, B. (2016). Structural diversity and biological activities of indole diketopiperazine alkaloids from fungi. *J. Agric. Food Chem.* 64, 6659–6671. doi: 10.1021/acs.jafc.6b01772

Meng, L. H., Li, X. M., Lv, C. T., Huang, C. G., and Wang, B. G. (2014). Brocazines a-f, cytotoxic bisthiodiketopiperazine derivatives from *Penicillium brocae* MA-231, an endophytic fungus derived from the marine mangrove plant *Avicennia marina*. *J. Nat. Prod.* 77, 1921–1927. doi: 10.1021/np500382k

Meng, L. H., Li, X. M., Lv, C. T., Li, C. S., Xu, G. M., Huang, C. G., et al. (2013). Sulfur-containing cytotoxic curvularin macrolides from *Penicillium sumatrense* MA-92, a fungus obtained from the rhizosphere of the mangrove *Lumnitzera racemosa*. *J. Nat. Prod.* 76, 2145–2149. doi: 10.1021/np400614f

Newman, D. J., and Cragg, G. M. (2020). Natural products as sources of new drugs over the nearly four decades from 01/1981 to 09/2019. *J. Nat. Prod.* 83, 770–803. doi: 10.1021/acs.jnatprod.9b01285

Peng, J. X., Gao, H. Q., Li, J., Ai, J., Geng, M. Y., Zhang, G. J., et al. (2014). Prenylated indole diketopiperazines from the marine-derived fungus *Aspergillus versicolor*. *J. Org. Chem.* 79, 7895–7904. doi: 10.1021/jo5010179

Perrone, G., and Susca, A. (2017). *Penicillium* species and their associated mycotoxins. *Methods Mol. Biol.* 1542, 107–119. doi: 10.1007/978-1-4939-6707-0_5

Phainuphong, P., Rukachaisirikul, V., Tadpetch, K., Sukpondma, Y., Saithong, S., Phongpaichit, S., et al. (2017). γ-Butenolide and furanone derivatives from the soil-derived fungus *Aspergillus sclerotiorum* PSU-RSPG178. *Phytochemistry* 137, 165–173. doi: 10.1016/j.phytochem.2017.02.008

Qiu, P., Cai, R. L., Lin, L., and She, Z. G. (2020). Three new isocoumarin derivatives from the mangrove endophytic fungus *Penicillium* sp. YYSJ-3. *Chin. J. Nat. Med.* 18, 256–260. doi: 10.1016/S1875-5364(20)30031-5

Quang, T. H., Lee, D. S., Sohn, J. H., Kim, Y. C., and Oh, H. (2013). A new deoxyisoaustamide derivative from the marine-derived fungus *Penicillium* sp. JF-72. *Bull. Korean Chem. Soc* 34, 3109–3112. doi: 10.5012/bkcs.2013.34.10.3109

Ren, J. W., Huo, R. Y., Liu, G. R., and Liu, L. (2021). New andrastin-type meroterpenoids from the marine-derived fungus *Penicillium* sp. *Mar. Drugs* 19, 189–197. doi: 10.3390/md19040189

Silva, G. H., Zeraik, M. L., de Oliveira, C. M., Teles, H. L., Trevisan, H. C., Pfenning, L. H., et al. (2017). Lactone derivatives produced by a *Phaeoacremonium* sp., an endophytic fungus from *Senna spectabilis*. *J. Nat. Prod.* 80, 1674–1678. doi: 10.1021/acs.jnatprod.5b00828

Song, T. F., Chen, M. X., Ge, Z. W., Chai, W. Y., Li, X. C., Zhang, Z. Z., et al. (2018). Bioactive penicipyrrodiether a, an adduct of GKK1032 analogue and phenol a derivative, from a marine-sourced fungus *Penicillium* sp. ZZ380. *J. Org. Chem.* 83, 13395–13401. doi: 10.1021/acs.joc.8b02172

Song, F. H., Liu, X. R., Guo, H., Ren, B., Chen, C. X., Piggott, A. M., et al. (2012). Brevianamides with antitubercular potential from a marine-derived isolate of *Aspergillus versicolor*. *Org. Lett.* 14, 4770–4773. doi: 10.1021/ol302051x

Steyn, P. S. (1973). The structures of five diketopiperazines from *Aspergillus ustus*. *Tetrahedron* 29, 107–120. doi: 10.1016/S0040-4020(01)99384-6

Sun, Y. B., Xia, G. Y., Xia, H., Wu, Y. Z., Wang, L. Y., and Lin, S. (2021). A new phenolic acid ester from solid culture of *Colletotrichum capsici*, an endophytic fungus from *Paeonia lactiflora*. *Chin. J. Chin. Mater. Med.* 46, 2837–2842. doi: 10.19540/j.cnki.cjcmm.20210402.201

Wang, Y. N., Tian, L., Hua, H. M., Lu, X., Sun, S., Wu, H. H., et al. (2009). Two new compounds from the broth of the marine fungus *Penicillium griseofulvum* Y19-07. *J. Asian Nat. Prod. Res.* 11, 912–917. doi: 10.1080/10286020903219923

Wohlgemuth, V., Kindinger, F., Xie, X. L., Wang, B. G., and Li, S. M. (2017). Two prenyltransferases govern a consecutive prenylation cascade in the biosynthesis of echinulin and neoechinulin. *Org. Lett.* 19, 5928–5931. doi: 10.1021/acs.orglett.7b02926

Xu, J. (2015). Bioactive natural products derived from mangrove associated microbes. *RSC Adv.* 5, 841–892. doi: 10.1039/C4RA11756E

Yang, J., Gong, L. Z., Guo, M. M., Jiang, Y., Ding, Y., Wang, Z. J., et al. (2021). Bioactive indole diketopiperazine alkaloids from the marine endophytic fungus *Aspergillus* sp. YJ191021. *Mar. Drugs* 19, 157. doi: 10+.3390/md19030157

Zhang, Y., Li, X. M., Shang, Z., Li, C. S., Ji, N. Y., and Wang, B. G. (2012). Meroterpenoid and diphenyl ether derivatives from *Penicillium* sp. MA-37, a fungus isolated from marine mangrove rhizospheric soil. *J. Nat. Prod.* 75, 1888–1895. doi: 10.1021/np300377b

Zhang, R. H., Zhang, J. X., Huo, R. Y., Xue, Y. X., Hong, K., and Liu, L. (2022). Sulfur-containing benzofurans and α-pyrones from the mangrove-derived fungus *Talaromyces* sp. WHUF0341. *Front. Mar. Sci.* 9. doi: 10.3389/fmars.2022.1034945

Zhou, L. M., Kong, F. D., Fan, P., Ma, Q. Y., Xie, Q. Y., Li, J. H., et al. (2019). Indole-diterpenoids with protein tyrosine phosphatase inhibitory activities from the marine-derived fungus *Penicillium* sp. KFD28. *J. Nat. Prod.* 82, 2638–2644. doi: 10.1021/acs.jnatprod.9b00620

Zhu, J. J., Huang, Q. S., Liu, S. Q., Ding, W. J., Xiong, Y. H., and Li, C. Y. (2022). Four new diphenyl ether derivatives from a mangrove endophytic fungus *Epicoccum sorghinum*. *Chin. J. Nat. Med.* 20, 537–540. doi: 10.1016/S1875-5364(22)60171-7

Zhuravleva, O. I., Antonov, A. S., Trang, V. T. D., Pivkin, M. V., Khudyakova, Y. V., Denisenko, V. A., et al. (2021). New deoxyisoaustamide derivatives from the coral-derived fungus *Penicillium dimorphosporum* KMM 4689. *Mar. Drugs* 19, 32. doi: 10.3390/md19010032